

ELECTROWEAK PHYSICS: W AND Z PRODUCTION AND STANDARD MODEL HIGGS SEARCH FROM THE FERMILAB TEVATRON

Abid Patwa^{1,2}

¹for the CDF and D \emptyset Collaborations,

²Department of Physics, Brookhaven National Laboratory,
Upton, New York 11973, USA

Abstract. This paper reviews recent measurements by the D \emptyset and CDF collaborations in $p\bar{p}$ collisions at the Fermilab Tevatron at $\sqrt{s} = 1.96$ TeV of W and Z boson production cross sections and asymmetries. Results from both experiments for the search of the Higgs boson predicted by the standard model in four different decay channels are also presented.

1 Introduction

Production of W and Z bosons in high energy $p\bar{p}$ collisions has been precisely predicted by the standard model (SM). Experimental measurements of their production cross sections not only allow for stringent tests of the SM but also serve as a means to understand detector performance. At hadron colliders, the hadronic decays of the W and Z tend to be overwhelmed by large QCD backgrounds and W and Z signatures can instead be efficiently identified through their leptonic decays. This abundant source of high p_T leptons also enables one to understand backgrounds for other important physics processes such as those in top, Higgs and SUSY decays.

Moreover, the Higgs boson is the only particle predicted in the standard model that has not yet been discovered. It is introduced in the SM in order to explain the mechanism of electroweak symmetry breaking. Experimental constraints provide considerable insight to its mass, which is a free parameter in the SM. Direct searches by the LEP experiments¹ yield a lower limit of 114.4 GeV at 95% C.L. on its mass while electroweak global fits give a 95% C.L. upper bound at 219 GeV². Present measurements of the W and top mass further constrain the Higgs mass via radiative corrections and tend to favor a relatively light mass, placing it within the anticipated sensitivity range of present collider experiments. Thus, the search for the Higgs is an integral part of the physics program at the Fermilab Tevatron experiments, CDF and D \emptyset .

This paper discusses measurements by CDF and D \emptyset of the W and Z production cross sections in their leptonic decay channels and a recent result of the W charge asymmetry by D \emptyset . Higgs searches within the SM in four different decay channels are also described. By the winter of 2005-2006, both CDF and D \emptyset have each recorded an integrated luminosity of over 1 fb^{-1} . The results presented here use up to 0.4 fb^{-1} of this dataset.

2 W and Z Production Cross Sections

Leptonic signatures of W boson decays are characterized by an isolated, energetic lepton with substantial missing transverse energy whereas Z boson decays contain two isolated, energetic

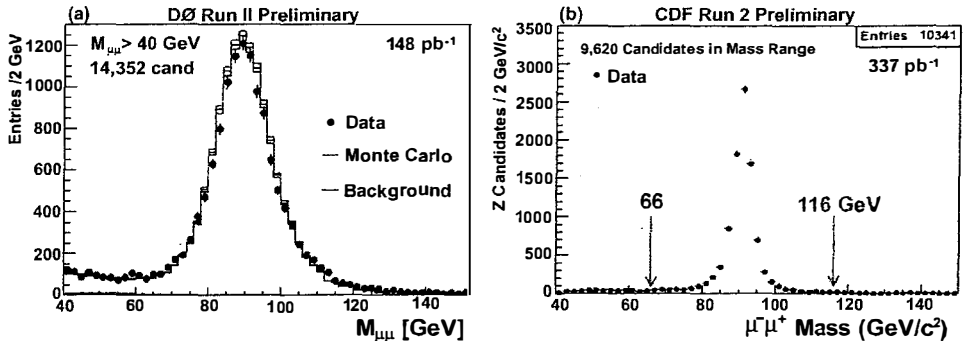


Figure 1: $Z \rightarrow \mu\mu$ invariant mass distribution for cross section measurements by (a) D0 and (b) CDF.

leptons of opposite charge. D0 and CDF each use a very similar selection technique in detecting electrons (e) decaying from the W and Z . Events must initially pass a single or di-electron trigger. Offline, at least one electron with $p_T > 25 \text{ GeV}$ must lie within the central fiducial volume of the detector ($|\eta| < 1.0$) and, for the W candidates, must have $\cancel{E}_T > 25 \text{ GeV}$. For the 2nd electron from Z candidates, D0 imposes very similar requirements as that of the 1st electron whereas CDF increases its electron acceptance to $|\eta| < 2.8$. Using 72 pb^{-1} integrated luminosity, CDF has selected 37,584 W and 4,242 Z boson candidates. D0 has analyzed a 177 pb^{-1} data sample, which yields 116,569 W and 4,625 Z boson candidates. The difference in number of events is largely due to the different integrated luminosities between the experiments.

Recently, CDF has also updated its $W \rightarrow e\nu$ cross-section measurement in the rapidity region $1.1 < |\eta| < 2.8$. Using the end-plug calorimeter and the ability to reconstruct 3D tracks at large η with the SVXII silicon detector, the measurement studies W reconstruction and properties in the forward region. Here, with an integrated luminosity of 223 pb^{-1} , 48,144 W boson candidates are selected.

For W and Z bosons decaying to muons (μ), both CDF and D0 select events that pass either a single or di-muon trigger and offline, require an isolated track in their muon system matched to a track in the central tracking system. Muons from W candidates must have $p_T > 20 \text{ GeV}$ and $\cancel{E}_T > 20 \text{ GeV}$. For Z candidates, CDF selects muons of $p_T > 20 \text{ GeV}$, both within $|\eta| < 1.0$. On the other hand, D0 requires each muon to satisfy $p_T > 15 \text{ GeV}$ and takes advantage of the wider acceptance of its muon chambers by including μ 's up to $|\eta| = 2.0$. CDF selects 57,109 W boson events using a 194 pb^{-1} data sample and 9,620 Z boson events from a 337 pb^{-1} sample. D0 selects 62,285 W candidates from a 96 pb^{-1} sample and 14,352 Z candidates from a 148 pb^{-1} dataset. Figure 1 shows the invariant mass for Z boson candidates after applying selection requirements. The larger number of D0 events indicates the increased acceptance of its muon system while the narrower peak in CDF's invariant mass distribution of muon pairs demonstrates the higher CDF tracking resolution.

CDF has updated its production cross section measurement in the $Z \rightarrow \tau\tau$ channel with 350 pb^{-1} of integrated luminosity. Since τ leptons decay a short distance before reaching any detector into a) $e\nu_e\nu_\tau$, b) $\mu\nu_\mu\nu_\tau$, or c) hadrons $+\nu_\tau$, effective τ identification algorithms must be used to discriminate between real taus (consisting of either charged leptons or narrow jets) with backgrounds dominated by jets produced by strong interaction processes. CDF reconstructs τ candidates as narrow, isolated energy clusters in the calorimeter associated with charged tracks. Next, π^0 information is added such that the invariant mass of the π^0 and the matched track-calorimeter cluster is consistent with the τ mass.

Reconstructing $Z \rightarrow \tau\tau$ candidates, CDF uses the channel where one τ decays into an

electron and the other decays hadronically. Event selections initially require one good quality isolated electron with $E_T^e > 10$ GeV and one hadronic tau candidate with $E_T^\tau > 15$ GeV, both in the central part of the detector, $|\eta_{e,\tau}| < 1.0$. In order to suppress QCD and W +jet backgrounds, event topology cuts are imposed. Figure 2 shows the track multiplicity distribution for observed hadronic taus and the expected backgrounds. A total of 504 $Z \rightarrow \tau\tau$ candidate events pass the selection requirements with a 37% QCD background estimate.

After all event selections, CDF and DØ calculate the product of W and Z production cross sections and branching ratios ($\sigma \times BR$) for each leptonic decay mode. The results are summarized in Table 1. At present, the accuracies are limited primarily by systematic effects extending from a) lepton identification (for e, μ : ~1-2%, for τ : ~3-4%), b) use of PDF (~1-2%), and c) background estimation (for e, μ : < 1%, for τ : ~4-5%). In general, the $\sigma \times BR$ measurement uncertainties are dominated by the uncertainty on the luminosity measurement, which is 6.0% (CDF) and 6.5% (DØ). All measurements are in agreement with NNLO theoretical calculations³. Using the ratio $\sigma_W \times BR/\sigma_Z \times BR$, one can extract the total width of the W boson, Γ_W^{tot} . Both the CDF and DØ result, also listed in Table 1, are in agreement with the SM value. Moreover, the CDF result for $\sigma_W \times BR(W \rightarrow e\nu)$ at forward rapidities is also consistent with their measurement in the central region. The CDF $W \rightarrow e\nu$ and $Z \rightarrow ee$ measurements with the 72 pb^{-1} data have been published⁴. DØ's $\sigma_Z \times BR(Z \rightarrow \tau\tau)$ measurement, also given in Table 1, has been published⁵.

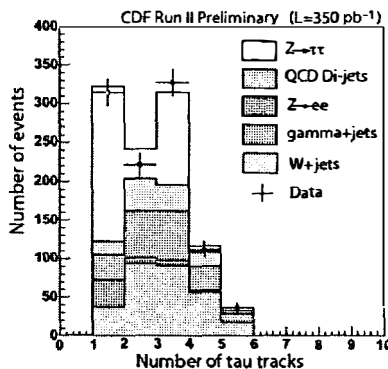


Figure 2: Track multiplicity distribution for a tau candidate in $Z \rightarrow \tau\tau$ events at CDF.

3 W Production Charge Asymmetry

Many electroweak measurements such as the W mass measurement at hadron colliders depend on the theoretical calculation of the W and Z cross sections or their transverse momentum distributions. At present, the precision of these quantities is limited by the uncertainties in the parton distribution functions (PDFs) used in these calculations. Studies of the W production charge asymmetry probes PDFs and can help provide new PDF constraints.

In a $p\bar{p}$ collider, the primary production mode of W^\pm bosons is $u + \bar{d} \rightarrow W^\pm$. The u quark carries more momentum than the \bar{d} quark causing the W^+ boson to be boosted in the proton direction and similarly, the W^- boson is boosted in the anti-proton direction. This results in a forward-backward charge asymmetry in the rapidity distribution for positive and negative W bosons. Since the longitudinal component of the neutrino from the W cannot be measured, the four momentum of the W cannot be fully reconstructed. Alternatively, the observable quantity is the lepton (ℓ) charge asymmetry, which is a convolution of the W production asymmetry and

Table 1: Summary of Tevatron $\sigma_{W,Z} \times BR$ and indirect Γ_W^{tot} measurements.

	$\sigma_{W,Z} \times BR \pm stat \pm sys \pm lum$ [in pb] ($\int \mathcal{L} dt$)	
	DØ	CDF
$W \rightarrow \mu\nu_\mu$	$2989 \pm 15 \pm 81 \pm 194$ (96 pb $^{-1}$)	$2786 \pm 12^{+69}_{-55} \pm 166$ (194 pb $^{-1}$)
$Z \rightarrow \mu\mu$	$291 \pm 3.0 \pm 6.9 \pm 18.9$ (148 pb $^{-1}$)	$261.2 \pm 2.7^{+5.8}_{-6.1} \pm 15.1$ (337 pb $^{-1}$)
$W \rightarrow e\nu_e$	$2865 \pm 8.3 \pm 76 \pm 186$ (177 pb $^{-1}$)	$2780 \pm 14 \pm 60 \pm 167$ (72 pb $^{-1}$, central)
		$2815 \pm 13^{+94}_{-89} \pm 169$ (223 pb $^{-1}$, end-plug)
$Z \rightarrow ee$	$264.9 \pm 3.9 \pm 9.9 \pm 17.2$ (177 pb $^{-1}$)	$255.8 \pm 3.9 \pm 5.5 \pm 15.4$ (72 pb $^{-1}$)
$\sigma_W/\sigma_Z \pm stat \pm sys$ $\Rightarrow \Gamma_W^{tot}$	$10.82 \pm 0.16 \pm 0.28$ $\Rightarrow 2098 \pm 74$ MeV	$10.92 \pm 0.15 \pm 0.14$ $\Rightarrow 2079 \pm 41$ MeV
	2092.1 ± 2.5 MeV	
$W \rightarrow \tau\nu_\tau$	—	$2620 \pm 7.0 \pm 210 \pm 160$ (72 pb $^{-1}$)
$Z \rightarrow \tau\tau$	$237 \pm 15 \pm 18 \pm 15$ (226 pb $^{-1}$)	$265 \pm 20 \pm 21 \pm 15$ (350 pb $^{-1}$)

the V-A decay of the W . Since the latter is well understood, the charge asymmetry factors into u and d PDF, defined by

$$A(\eta_e) = \frac{d\sigma(\ell^+)/d\eta - d\sigma(\ell^-)/d\eta}{d\sigma(\ell^+)/d\eta + d\sigma(\ell^-)/d\eta} \simeq \frac{d(x)}{u(x)} \quad (1)$$

DØ has recently measured the W charge asymmetry in the $W \rightarrow \mu\nu$ channel with a 230 pb $^{-1}$ sample of data. Since the phase space for the measurement at tree-level is limited by the range of W boson rapidity that can be reconstructed, widest η coverage is essential. The large rapidity coverage of the DØ muon detectors together with forward muon triggers enables the asymmetry to be measured up to $|\eta| = 2.0$. Event selections require a single isolated muon with large missing transverse energy from the neutrino, similar to those used in the $W \rightarrow \mu\nu$ cross section measurement. Proper charge identification is critical for the measurement; DØ imposes track quality requirements to improve the charge-id rate and measures the mis-id probability at 0.01% for $|\eta| \sim 2.0$. Figure 3a shows the measured muon charge asymmetry distribution corrected for background effects. At large η , the measurement is statistically limited, and in order to improve the statistical uncertainties, the asymmetry is CP folded, as shown in Figure 3b. Also overlaid in Figure 3 are the MRST02 PDF central value⁶ and the CTEQ6.1M PDF $\pm 1\sigma$ error bands⁷. A comparison between each indicates that DØ's result can be used to help constrain future PDFs.

4 SM Higgs Searches

Tevatron searches for the Higgs (H) boson expected within the standard model rely on two basic search strategies. For light mass Higgs ($M_H < 135$ GeV), the dominant production mode is via gluon fusion, where the Higgs subsequently decays into a $b\bar{b}$ jet final state. Since this mode tends to be overwhelmed with multijet backgrounds, the search instead looks for the Higgs produced

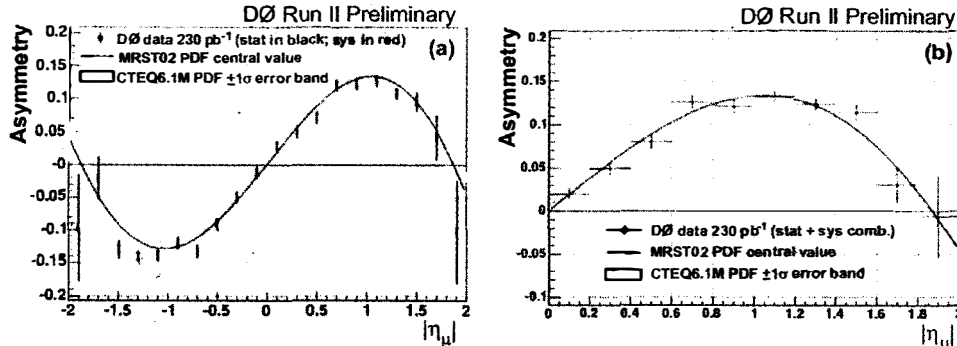


Figure 3: DØ's measurement of (a) $W \rightarrow \mu\nu$ charge asymmetry and (b) with CP folding. Shown with the data (points) are the CTEQ6.1 PDF $\pm 1\sigma$ error band (yellow, shaded) and the central MRST02 PDF value (blue curve).

in association with either a W or Z boson. The final state consists of leptons from the W or Z in addition to two b -jets from the Higgs. Such analyses exploit efficient lepton identification and b -tagging techniques. For higher mass Higgs ($M_H > 135$ GeV), searches which give the most sensitivity concentrate on Higgs production via gluon fusion and its decay into two gauge bosons, primarily WW . The studies hinge around reconstruction of leptons from the WW .

4.1 $WH \rightarrow \ell\nu b\bar{b}$ Search Channel

CDF and DØ use very similar methods to search for the associated production of the Higgs with a W boson. DØ studies the channel $WH \rightarrow e\nu b\bar{b}$. Meanwhile, CDF not only studies the electron channel but also focuses on $WH \rightarrow \mu\nu b\bar{b}$. The experimental signature requires a final state with one high E_T lepton (DØ: $E_T^e > 20$ GeV, CDF: $E_T^e > 20$ GeV or $p_T^\mu > 20$ GeV), two b -jets, and significant missing transverse energy (DØ: $\cancel{E}_T > 25$ GeV, CDF: $\cancel{E}_T > 20$ GeV). CDF selects events with at least one tagged b -jet while DØ imposes a tighter condition where the second b -jet must also be tagged. The dominant backgrounds to WH production are from W +heavy flavor, $t\bar{t}$, and single-top quark production. Using a dataset of 382 pb^{-1} at DØ and 319 pb^{-1} at CDF, each experiment looks for a resonant mass peak in the dijet mass spectrum, as shown in Figure 4. In order to limit the $Wb\bar{b}$ background contribution, the search is restricted to optimized $b\bar{b}$ invariant mass intervals, which vary with the Higgs masses studied. For $M_H = 115$ GeV, DØ observes 4 events in a dijet mass window of $85 < M_{bb} < 135$ GeV, and the expected SM background is 2.37 ± 0.59 . Similarly, CDF observes 14 events with a 14.62 ± 3.25 expected background. Across the different Higgs masses, both experiments find the signal to be consistent with the expected backgrounds and set 95% C.L. upper limits on the cross section $\sigma_{WH} \times BR(H \rightarrow b\bar{b})$ at 7.6 to 6.9 pb (DØ) and 10 to 2.8 pb (CDF, single b -tag analysis) and 9.7 to 6.6 pb (CDF, double b -tag analysis). The results are shown in Figure 5.

4.2 $ZH \rightarrow \nu\bar{\nu} b\bar{b}$ Search Channel

Because of the large $Z \rightarrow \nu\bar{\nu}$ and $H \rightarrow b\bar{b}$ branching ratios, one sensitive way to search for a light Higgs is its associated production with a Z boson. At low masses, the product of cross section and branching fraction is expected to be on the order of 0.01 pb and comparable to that of $WH \rightarrow \ell\nu b\bar{b}$. Since the two b -jets from the Higgs boson decay are boosted along the Higgs momentum direction, the final state contains a distinct signature of acoplanar jets in contrast to typical back-to-back QCD dijets. The main backgrounds are from $W/Z+jets$, electroweak

diboson (WZ and ZZ) production, and $t\bar{t}$ processes where the lepton or jets escape. Multijets, where the jets are mismeasured and/or misidentified, dominate as instrumental backgrounds and contribute to the missing transverse energy measurement.

The D \emptyset event selections that help separate the signal from background require two b -tagged jets with $p_T > 20$ GeV, $\cancel{E}_T > 25$ GeV, no back-to-back event topology, and no isolated tracks in the event. The last three conditions suppress QCD multijet and $W/Z +$ jet background events. Additional track and asymmetry cuts developed using variables such as the vector sum of the p_T of all tracks, \cancel{E}_T , and H_T (the scalar sum of jet p_T) reduce the instrumental backgrounds.

Event selections by CDF consist of two b -jets, each with $E_T > 25$ GeV, and at most a third soft jet, which can be radiated off by one of the b -jets. While D \emptyset requires both jets to be tagged, CDF selects events with at least one b -tagged jet. Further, in order to limit the effect of jets or leptons being mismeasured, a $\cancel{E}_T > 70$ GeV condition is imposed. The data is subsequently divided into two control regions to understand the backgrounds: I) events with no high- p_T isolated leptons and azimuthal angular separation between the second leading jet and \cancel{E}_T , $\varphi(2^{nd} \text{ jet}, \cancel{E}_T) < 0.4$ and II) events with at least one lepton or isolated track and $\varphi(2^{nd} \text{ jet}, \cancel{E}_T) > 0.4$. Region I is dominated by QCD multijet events and Region II contains top and electroweak backgrounds. After comparing the data from these control regions to the simulated SM backgrounds, selections are optimized using variables defined by the E_T of the leading jet, H_T , and the angular separation between the leading jet and \cancel{E}_T .

Both D \emptyset (using 261 pb^{-1} dataset) and CDF (using 289 pb^{-1} dataset) search for a peak in the dijet invariant mass distribution. Since no significant excess is observed over expected backgrounds, 95% C.L. cross section upper limits are established at $\sigma_{ZHH} \times BR(H \rightarrow b\bar{b})$ of $7.7 - 12.2 \text{ pb}$ for Higgs masses between 105 and 135 GeV (D \emptyset) and $4.5 - 5.45 \text{ pb}$ between 90 and 135 GeV Higgs masses (CDF). These results also appear in Figure 5.

4.3 $H \rightarrow WW^{(*)}$ Search Channel

Standard model Higgs search in $H \rightarrow WW^{(*)}$, which subsequently decays into three final states: e^+e^- , $e^\pm\mu^\mp$, and $\mu^+\mu^-$ is the dominant production mechanism for higher mass Higgs. Such events are triggered by the presence of isolated, oppositely charged single or di-leptons. However, a Higgs search in this channel contains an exhaustive list of backgrounds: electroweak diboson (WW and WZ) production, Z/γ^* , ZZ , where one or two leptons are respectively mismeasured, multijets and $W +$ jets, where the jets are misidentified as leptons, and $t\bar{t}$ production.

Within this channel, both CDF and D \emptyset use a very similar search strategy that is based on

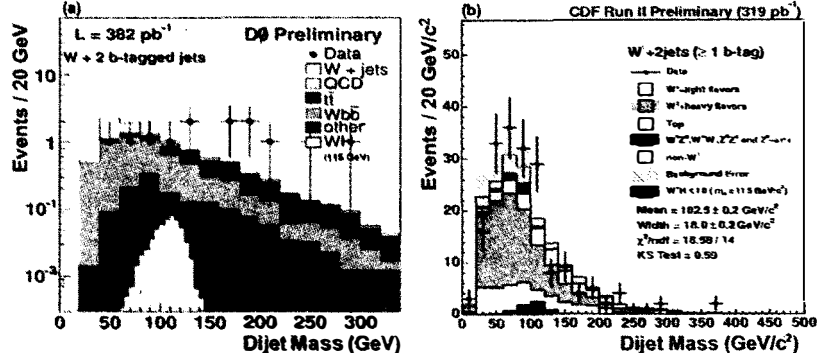


Figure 4: Dijet invariant mass distribution for Higgs search in WH channel by (a) D \emptyset and (b) CDF.

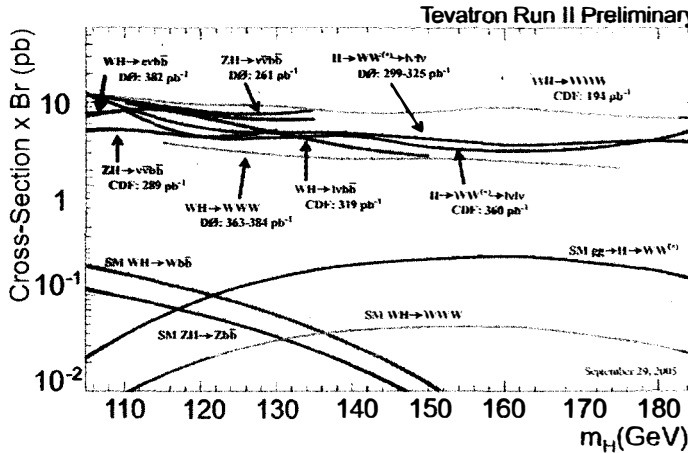


Figure 5: Summary of standard model Higgs boson searches at the Tevatron. Shown are the 95% C.L. production cross section upper-limits as a function of Higgs masses measured by CDF and D \emptyset across different Higgs channels.

the WW decay topology. Due to the scalar nature of the Higgs, the two charged leptons from the W are emitted in-parallel with small azimuthal angular separation ($\Delta\varphi_{ll} < 2.0$) between them, and in contrast to the standard back-to-back multijet background. Moreover, from W -helicity conservation, the lepton system and the neutrinos are emitted mostly back-to-back, which allow the dilepton invariant mass to be constrained to $M_H/2$. Selections based on two oppositely-charged high p_T leptons, large \cancel{E}_T from the ν 's, $\Delta\varphi_{ll}$, and dilepton invariant mass become an effective method in discriminating a Higgs signal from backgrounds. Once the selections have been optimized, the number of events observed by each experiment is consistent with those expected from backgrounds. As summarized in Figure 5, 95% C.L. production limits are therefore extracted for different Higgs masses. The limits are from a combination of all three decay channels using integrated luminosities of CDF: 360 pb^{-1} and D \emptyset : $325 \pm 21 \text{ pb}^{-1}$ (e^+e^-), $318 \pm 21 \text{ pb}^{-1}$ ($e^\pm\mu^\mp$), and $299 \pm 19 \text{ pb}^{-1}$ ($\mu^+\mu^-$). The D \emptyset result has been published⁸.

4.4 $WH \rightarrow WWW^{(*)}$ Search Channel

The search for associated Higgs production via the channel $WH \rightarrow WWW^{(*)} \rightarrow \ell^\pm\nu\ell^\pm\nu q\bar{q}$ is more promising than direct Higgs production, $H \rightarrow WW^{(*)}$, as it requires like-sign leptons and therefore, avoids large SM backgrounds from electroweak diboson and $t\bar{t}$ production, which contain oppositely charged leptons. Instead, the primary physics background is from $WZ \rightarrow \ell\ell\ell\ell$, where one of the leptons from the Z is lost. Instrumental backgrounds that contribute non-negligibly to this mode are a) dominated by mismeasuring the charge of one of the leptons in $Z/\gamma^* \rightarrow \ell\ell$ decays (often referred to as “charge flips” at D \emptyset) and b) QCD processes, which contain semileptonic heavy flavor decays, punch-through hadrons misidentified as muons, or $\gamma \rightarrow e$ conversions.

With $363-384 \text{ pb}^{-1}$ dataset, D \emptyset selects an event containing like-sign ee , $e\mu$, and $\mu\mu$ candidates with $p_T > 15 \text{ GeV}$ per lepton and $\cancel{E}_T > 20 \text{ GeV}$. Track quality cuts are imposed to reduce the charge flip probability. The background composition differs among the three channels. Because of the improved \cancel{p}_T measurement in the ee channel, the \cancel{E}_T cut is very effective in reducing QCD and charge flips and thus, the ee channel is dominated by the WZ physics background. In contrast, charge flips dominate the $\mu\mu$ channel (where $Z/\gamma^* \rightarrow \ell\ell$ production

is significant) and QCD contribute largely to the $e\mu$ channel. Nonetheless, D \emptyset observes 1 ee event, 3 $e\mu$ events, and 2 $\mu\mu$ events, all which are in agreement with the expected backgrounds.

CDF's present analysis based on an integrated luminosity of 194 pb^{-1} stems from simple techniques that require isolated like-sign leptons but do not use explicit selections on the signal such as \cancel{E}_T and other topological cuts. Instead, the data is divided into a signal and a series of control regions determined by the magnitude and vector sum of the first and second leading lepton p_T . No events are observed in the signal region, while the total background is expected to be 0.95 ± 0.80 .

Again, Figure 5 shows the 95% C.L. upper limits on the cross section as a function of different Higgs masses. Since no signal-specific cuts are introduced in the analysis, the present CDF result is conservative for the Higgs search. However, once further optimizations are done, sensitivity in this production mode seems very promising.

5 Conclusion

Using a fraction of the 1 fb^{-1} integrated luminosity, CDF and D \emptyset have measured the product of cross section and branching ratios in the different leptonic channels of W and Z boson production and all results are in agreement with standard model expectations. The measurements also lay the foundation for understanding not only the detector response but also backgrounds for other important physics processes.

Moreover, both CDF and D \emptyset have searched for the Higgs boson predicted in the standard model across a comprehensive set of search channels. In the absence of signal, each experiment has established 95% C.L. cross section upper limits. However, the analyses are presently trying to reach the sensitivity outlined by the 2003 Higgs Sensitivity Studies⁹. In particular, the current results from the Tevatron indicate the expected sensitivity has not been reached typically by a factor of 2–3. Several approaches such as optimizing analyses techniques, adding or combining search channels, and combining results from each experiment will help bridge the gap between the current limits and those predicted by the SM. Indeed, studies implementing some of these methods are already underway as are Higgs searches using the full 1 fb^{-1} of collected data. The Tevatron experiments look forward to the prospects for a light mass Higgs discovery with 4–8 fb^{-1} of integrated luminosity.

Acknowledgments

The author appreciates and wishes to thank the CDF and D \emptyset collaborations for useful discussions and providing the results presented here.

References

1. R. Barate et al., (The LEP Higgs Working Group), *Phys. Lett. B* **565**, 61 (2003).
2. The LEP Collaborations ALEPH, DELPHI, L3, OPAL, the LEP Electroweak Working Group, the SLD Electroweak and Heavy Flavor Groups. (URL: <http://lpcwwwg.wcb.cern.ch/LEPEWWG/>)
3. C.R. Hamberg, W.L. van Neerven and T. Matsuura, *Nucl. Phys. B* **359**, 343 (1991).
4. D. Acosta et al., (CDF Collaboration), *Phys. Rev. Lett.* **94**, 091803 (2005).
5. V. M. Abazov et al., (D \emptyset Collaboration), *Phys. Rev. D* **71**, 072004 (2005).
6. A. Martin, R. Roberts, W. Stirling, and R. Thorne, *Eur. Phys. J. C* **4**, 463 (1998).
7. J. Pumplin et al., *JHEP* **0207**, 012 (2002).
8. V. M. Abazov et al., (D \emptyset Collaboration), *Phys. Rev. Lett.* **96**, 011801 (2006).
9. CDF and D \emptyset Collaborations, hep-ph/0010338, FERMILAB-PUB-03/320-E (2003).